

# Experimental Test of the Cooperative Free Volume Rate Model under 1D Confinement: The Interplay of Free Volume, Temperature, and Polymer Film Thickness in Driving Segmental Mobility

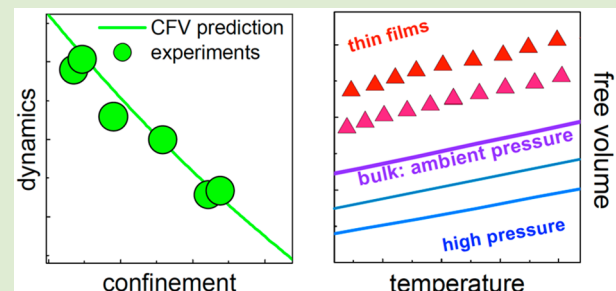
Alice Debot,<sup>†</sup> Ronald P. White,<sup>‡</sup> Jane E. G. Lipson,<sup>\*,‡,ID</sup> and Simone Napolitano<sup>\*,†,ID</sup>

<sup>†</sup>Polymer and Soft Matter Dynamics, Faculté des Sciences, Université libre de Bruxelles (ULB), Brussels, Belgium

<sup>‡</sup>Department of Chemistry, Dartmouth College, Hanover, New Hampshire 03755, United States

## Supporting Information

**ABSTRACT:** We show that the Cooperative Free Volume (CFV) rate model, successful at modeling pressure-dependent dynamics, can be employed to describe the temperature and thickness dependence of the segmental time of polymers confined in thin films (1D confinement). The CFV model is based on an activation free energy that increases with the number of cooperating segments, which is determined by the system's free volume. Here, we apply the CFV model to new experimental results on the segmental relaxation of 1D confined poly(4-chlorostyrene), P4CLS, and find remarkable agreement over the whole temperature and thickness ranges investigated. This work further validates the robustness of the CFV model, which relates the effects of confinement on dynamics to pressure changes in the bulk, and supports the idea that confinement effects originate from local perturbations in density.



Over the last three decades, significant experimental and theoretical efforts have been dedicated to understanding how the dynamics of liquids approaching the glass transition are affected by confinement at the nanoscale level.<sup>1–10</sup> The interest toward geometries having at least one dimension at the nanometer scale originated from the success of theories predicting a length scale of the glass transition on the order of 1–5 nm.<sup>11–15</sup>

Most of the studies on glassy dynamics under nanoconfinement are on thin polymer films because of the ease with which samples of well-defined size can be prepared. Thin polymer layers are stabilized, relative to small molecule samples, because of the higher mechanical moduli, the possibility to irreversibly adsorb onto solid substrates, even at monomer/wall interactions smaller than thermal energy, and the limited tendency toward crystallization.

The data collected so far indicate that the dynamics, experimentally parametrized via the characteristic time of density fluctuations,  $\tau$ , can either speed up, slow down, or be invariant upon confinement.<sup>1</sup> However, despite the tremendous efforts, no direct proof of finite size effects on the glassy dynamics of thin polymer films has been observed so far. On the other hand, results hint at an interfacial origin of the perturbations in the dynamics of thin films. Considering an experimentally accessible quantity characterizing the sample dynamics,  $X$ , for example,  $\log \tau$  or  $T_g$  (the dynamic glass transition temperature), the deviation from bulk behavior  $|X_{\text{film}} - X_{\text{bulk}}|$  increases with  $h^{-1}$ , the inverse of the sample thickness, which in the geometry of thin films corresponds to the surface/volume ratio.<sup>16</sup> Another feature further supporting the

interfacial nature of glassy dynamics in thin films is the reduction in  $|X_{\text{film}} - X_{\text{bulk}}|$  with increasing temperature, a trend also shared by inorganic materials.<sup>17</sup>

In this Letter, we show that the Cooperative Free Volume (CFV) rate model successfully describes  $\tau(T, h)$ , the temperature and thickness dependence of the segmental time of polymers confined in thin films (1D confinement). We apply the CFV model to new dielectric spectroscopy experimental results on the segmental relaxation of Al-capped poly(4-chlorostyrene) (P4CLS) films. This is a convenient system, having relatively strong shifts in dynamics and a high dielectric signal.<sup>18</sup> We note that the modeling therefore focuses on segmental ( $\alpha$ -) relaxation dynamics, and not the pseudothermodynamic  $T_g$ ; the two commonly show different experimental confinement behavior.<sup>1,8,9,19</sup> By using bulk data to characterize the pressure dependence of the segmental time and the isothermal thickness dependence of the segmental time at a single temperature, as input, the CFV model made testable predictions that, we show here, successfully anticipated the outcome of experiments over the whole temperature range investigated in this work.

Key results from this work are summarized as follows: (1) The predictions of the CFV model are quantitative. (2) The model captures the experimental  $\log \tau \sim 1/h$  trend and shows sensitivity to confinement decreases with increasing  $T$ . (3) The

Received: October 31, 2018

Accepted: December 18, 2018

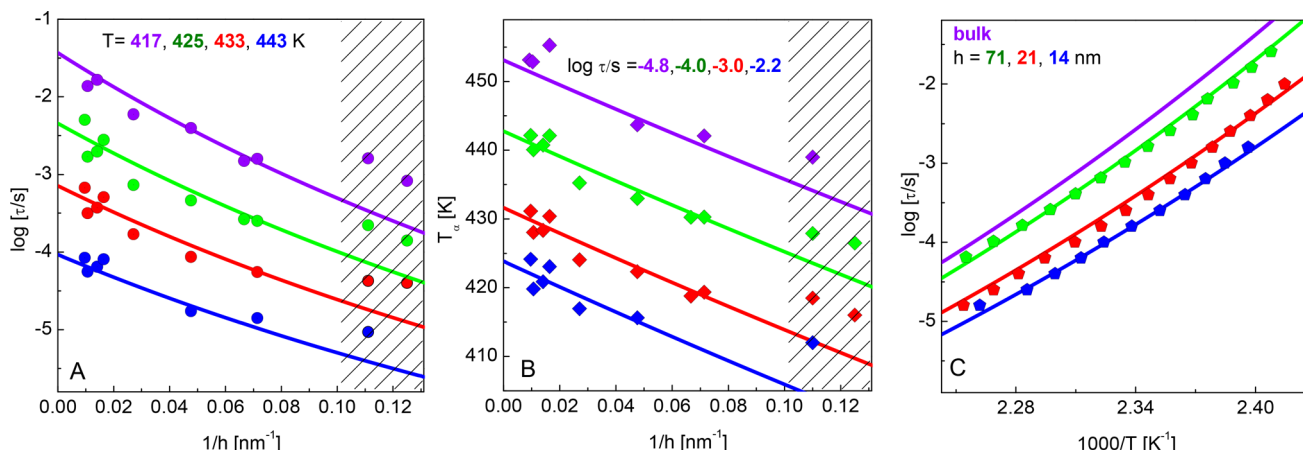


**Figure 1.** (A) Segmental relaxation times for P4CLIS films vs inverse thickness ( $1/h$ ) in isothermal conditions; (B) Dynamic glass transition temperature ( $T_g$ ) vs  $1/h$  in isochronal conditions (10 kHz, 1.6 kHz, 159 Hz, 1.6 Hz); (C) Temperature dependence of  $\tau$  for several films. Points indicate experimental data and curves the CFV  $\tau(T,h)$  model predictions. Error estimates are  $\leq 2$  K for  $T_g$  and  $\leq 0.15$  for  $\log \tau$ .

model describes the system's bulk pressure-dependent dynamics,  $\tau(T,V)$ , first, a key link to describing confinement,  $\tau(T,h)$ . (4) The connection to pressure dependence shows that confinement effects ( $1/h$  dependence and its thermal sensitivity) can be explained in terms of how bulk dynamics responds to changes in temperature and density. (5) The model has the ability to determine the free volume content of a film using  $\tau$  data as input and provides support for the idea that confinement effects originate from interfacial perturbations in density.

A key ingredient in CFV is the system's thermodynamically characterized free volume.  $V_{\text{free}}$  is defined as the difference between a system's overall volume,  $V$ , and its limiting, closely packed, hard core value,  $V_{\text{hc}}$ .

$$V_{\text{free}} = V - V_{\text{hc}} \quad (1)$$

$V_{\text{hc}}$  is a constant for each system, independent of both  $T$  and  $P$ . Its value is determined via analysis of experimental PVT data using the locally correlated lattice (LCL) model equation of state (EOS).<sup>20</sup> To extend our analysis to films, we consider that there can be more free space near an interface<sup>16,21</sup> and define a film-averaged relative free volume (details in ref 22). It is the result of a weighted average of a bulk-like region (which has a bulk-like free volume as determined via the LCL EOS analysis) and an interfacial region (which has enhanced free volume compared to bulk, to a degree that is manifest in a single parameter,  $\delta_{\text{free}}$ ). Films thus have more free volume compared to bulk, with a thickness-dependent average that is given by

$$\begin{aligned} (V_{\text{free}}/V_{\text{hc}})_{\text{film}} &= (V_{\text{free}}/V_{\text{hc}})_{\text{bulk}} + (\delta_{\text{free}}/h) \\ &= (V_{\text{free}}/V_{\text{hc}})_{\text{bulk}}^\circ + (T - T^\circ)(\alpha V/V_{\text{hc}})_{\text{bulk}}^\circ + (\delta_{\text{free}}/h) \end{aligned} \quad (2)$$

The thermal expansion of films under ambient pressure conditions is written relative to the conditions at a reference temperature,  $T^\circ$  (see below).

The CFV rate model<sup>23,24</sup> describes segmental relaxation times under general pressure-dependent conditions,  $\tau(T,V)$ . It is based on a cooperative picture where the total activation free energy,  $\Delta A_{\text{act}} = n^* \Delta a$ , changes with the number,  $n^*$ , of cooperating segments. In CFV, it is the system's free volume that determines  $n^*$ , giving a general form

$$\tau = \tau_{\text{ref}} \exp \left[ n^* \times \left( \frac{\Delta a}{T} \right) \right] = \tau_{\text{ref}} \exp \left[ \left( \frac{1}{V_{\text{free}}} \right) \times f(T) \right] \quad (3)$$

where  $n^* \propto 1/V_{\text{free}}$  depends inversely on free volume, and  $\Delta a$  is the activation free energy per cooperating segment (which is independent of volume).  $V_{\text{free}}$  controls the volume-based contribution to the dynamics. In practice, a  $T$ -dependence,  $f(T) \sim 1/T^b$ , is found via connection to thermodynamic scaling approaches,<sup>25-27</sup> and this leads to the main CFV working expression,

$$\ln \tau = \left( \frac{V_{\text{hc}}}{V_{\text{free}}} \right) \left( \frac{T^*}{T} \right)^b + \ln \tau_{\text{ref}} \quad (4)$$

where  $b, T^*$ , and  $\tau_{\text{ref}}$  are parameters (see below).

When the expression for the film-averaged free volume (eq 2) is substituted into the main CFV dynamics equation (eq 4), we obtain the model expression (eq 5) below (see ref 22), which yields  $\tau(T,h)$  for films at ambient pressure,

$$\ln \tau = \frac{(T^*/T)^b}{(V_{\text{free}}/V_{\text{hc}})_{\text{bulk}}^\circ + (T - T^\circ)(\alpha V/V_{\text{hc}})_{\text{bulk}}^\circ + (\delta_{\text{free}}/h)} + \ln \tau_{\text{ref}} \quad (5)$$

Details on the model parametrization can be found in the **Supporting Information**. Briefly, the dynamics-related parameters,  $b$ ,  $T^*$ , and  $\tau_{\text{ref}}$  (appearing in eqs 4 and 5), are determined by fitting eq 4 (with  $b$  fixed) to ambient bulk dynamics data along with information from PVT data (that gave  $b$ , a priori). The thermodynamics-based parameter,  $V_{\text{hc}}$ , and the values of  $(V_{\text{free}}/V_{\text{hc}})_{\text{bulk}}^\circ$  and  $(\alpha V/V_{\text{hc}})_{\text{bulk}}^\circ$  ( $\alpha$  is the coefficient of thermal expansion) for the chosen  $T^\circ$  were calculated from the LCL EOS analysis of the equilibrium PVT data. The interface-related parameter,  $\delta_{\text{free}}$ , was determined using dynamics data on the P4CLIS film. Note that this  $\delta_{\text{free}}$  value was based on data at just a single temperature, yet, in this work, we will now use this same single  $\delta_{\text{free}}$  to describe the film behavior over all  $T$ .

In ref 22, experimental P4CLIS film data<sup>18</sup> were available at only a single temperature ( $T = 433$  K). This was still enough to completely characterize the model  $\tau(T,h)$  expression and yielded testable predictions involving the temperature dependence of the film behavior. For example, we considered the isochronal " $T_g$ " behavior, the thickness-dependent temperature

at which films show the same  $\tau$  value (analogous to the dynamic  $T_g$ ). We predicted that the  $T_\alpha$  suppression (relative to bulk) would be about 13 K for a 14 nm film. Here we test this result and find, indeed, a  $T_\alpha$  suppression of  $12 \pm 2$  K. These predictions turn out to be quantitative to within the experimental error.

A broad set of experimental  $T, h$ -dependent relaxation time results are compared to the corresponding model  $\tau(T, h)$  behavior in Figure 1, where the three panels show three cuts through the general  $\tau(T, h)$  space. Panel B shows the model-data agreement on  $T_\alpha$  versus  $1/h$  isochrones (several constant  $\tau$  values). Panel A shows  $\log \tau$  versus  $1/h$  isotherms (constant  $T$  cuts), and panel C shows  $\log \tau$  versus  $1/T$  for several chosen film thicknesses (constant  $h$  cuts). The agreement between CFV predictions and new experimental data is excellent.

The model is expected to breakdown for films where no bulk-like region is present. (Details are in the appendix of ref 22.) For these extremely thin films, eq 2 for the film's weighted average  $V_{\text{free}}$  is no longer valid. The new results here show that the location of this breakdown point is around  $h \leq 10$  nm. The model prediction for the 8 and 9 nm films (Figure 1A,B) is well outside the error associated with the experimental data. With two experimental surfaces, the CFV model indicates that the interfacial region must be roughly 5 nm wide, in line with the value obtained via adsorption experiments.<sup>18</sup>

The CFV model passes a stringent test to cover the independent changes in  $T$  and  $h$ ; this is analogous to the essential requirement in  $P$ -dependent modeling,<sup>25,26</sup> where one must account for independent changes in  $T$  and  $V$ . Indeed, the fact that CFV describes a system's bulk  $P$ -dependent dynamics data is what then provides it the ability to model confinement, because changing film thickness and changing density (free volume) are related. In addition to films, the importance of bulk  $P$ -dependent analysis has been clearly demonstrated in recent nanopore studies.<sup>28–30</sup>

The CFV film model accounts for a film's relaxation behavior by enacting its  $h$ -dependence within the (free) volume contribution. With film data only at a single temperature, it may be the case that a fitted value of the  $\delta_{\text{free}}$  parameter could possibly compensate for an incorrect model  $h$ -dependence (e.g., through ignoring the role of a film's ambient thermal expansion, or, incorrectly placing the  $h$  dependence in the independent  $T$ -based contribution). However, our test here of the model predictions over a range in  $T$  shows that a single value for  $\delta_{\text{free}}$  works, meaning that the ( $h$ ) confinement effect indeed resides in (only) the volume contribution. This supports our explanation that the effect of an interface is traceable to the change it induces in density and that it is this density change that causes the change in dynamics.

Note that if a direct intermolecular energetic interaction effect were important in confinement, these altered molecular interactions would lead to altered activation energies. The result would have been an altered  $T$ -dependence, and we would not have been able to simply use the bulk CFV ( $T^*/T$ )<sup>b</sup> term as the independent  $T$ -contribution. The results here show that the bulk  $T$ -contribution is sufficient. Thus, we can now say that at least for P4C1S, the confinement effect owes its direct origin to changes in density. Interfacial interactions undoubtedly play an indirect role, since they induce the density change that impacts the dynamics. The nature and strength of these interactions will differ from system to system and are characterized by the  $\delta_{\text{free}}$  value.

We therefore now consider explicitly the free volume behavior of films. The model expression for the  $V_{\text{free}}$  of a film was given in eq 2: the difference compared to bulk is proportional to  $1/h$ , and the  $T$ -dependence (expansion rate,  $\alpha$ ) of the ambient film is the same as that for ambient bulk. (By contrast, nanopore experiments<sup>28–31</sup> give rise to isochoric conditions.) Support for the eq 2 form is shown by the agreement in Figure 1.

However, it is also instructive to consider what would result by making no assumptions about the  $T, h$  form. This can be explored by back-calculating  $V_{\text{free}}$  values from the more general CFV equation for  $P$ -dependent dynamics (eq 4), which has been parametrized to predict the bulk P4C1S  $P$ -dependent behavior. Here we input the measured experimental  $\tau$  value and experimental temperature and solve eq 4 for  $V_{\text{free}}$ . The results are shown in Figure 2, where we plot the relative free

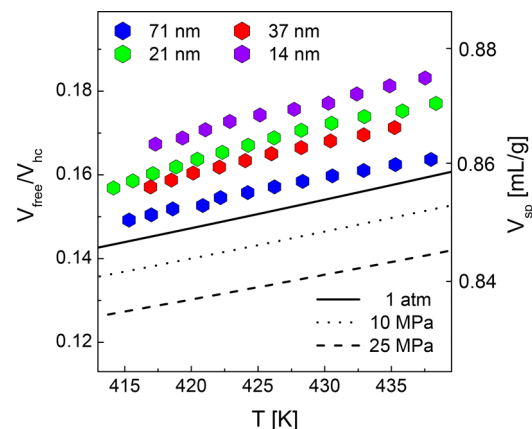


**Figure 2.** Relative free volume ( $V_{\text{free}}/V_{\text{hc}}$ ) and corresponding specific volume of P4C1S films as a function of temperature, calculated from CFV, eq 4, based on experimental relaxation times. The LCL EOS-based  $V_{\text{free}}/V_{\text{hc}}$  and specific volume for the P4C1S bulk melt at ambient pressure and two higher pressure isobars are shown for comparison. The relative error in  $V_{\text{free}}/V_{\text{hc}}$  is smaller than 1.5%.

volume for films (at ambient pressure) as a function of temperature for several choices of film thickness, along with the LCL results for the P4C1S bulk  $V_{\text{free}}(T)$  at ambient pressure, as well as two values of higher pressure for comparison.

Our simple definition of free volume allows us to easily translate our free volume values (via eq 1) into the corresponding experimental density (or specific volume). Therefore, we also show the system specific volume on the right-hand  $y$ -axis of Figure 2. The results in the figure show that, compared to ambient bulk, the change (increase) in  $V_{\text{free}}$  for a roughly 15 nm film (14 and 21 nm films are shown) is comparable in magnitude to the change (decrease) in  $V_{\text{free}}$  that the bulk would experience when the pressure is increased by about 25 MPa or so. Compared to the amount of free space available in the ambient bulk, the 14 nm film has roughly 14% more free space, and, going in the other direction, the bulk at  $P = 25$  MPa has about 12% less. Quoting these values in terms of density at 433 K, the ambient bulk has  $\rho = 1.169$  g/mL (which increases to  $\rho = 1.188$  g/mL at  $P = 25$  MPa), while the 14 nm film has an effective average  $\rho = 1.146$  g/mL. This gives a density change of about 2% on going from ambient bulk to a 14 nm film. Direct experimental measurement of film density is a challenge, and results have varied.<sup>32,33</sup> However, changes in

average film density have been clearly seen in simulations,<sup>34</sup> and additional evidence comes from probe adsorption experiments.<sup>16,21</sup> Note in the model picture we expect the interior of the film to be bulk-like; it is the thin region around the edges that lowers the average density. (The appendix of ref 22 expands on this in detail.)

Note that the  $T$ -dependence of the back-calculated film free volumes shows the same average rate of expansion as the ambient bulk. These results demonstrate that the “fingerprint” of the material’s ambient volumetric behavior exists within the experimentally measured relaxation times. We conclude that the slopes of the back calculated film free volumes follow the bulk expansion rate because the confinement effect is driven by volumetric behavior and that the CFV model captures that successfully.

Lastly, we test the validity of the CFV prediction that the sensitivity to confinement,  $-(\partial \log \tau / \partial (1/h))_T$ , will decrease with increasing temperature. The experimental results here (Figure 3) are in quantitative agreement with the model. This

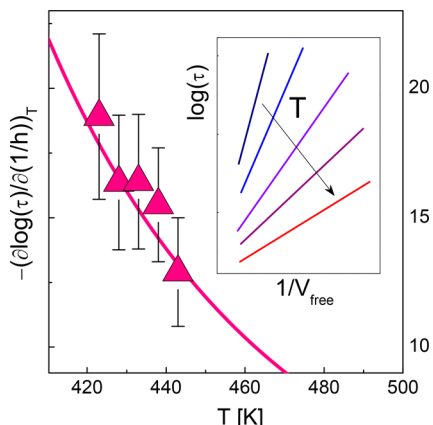


**Figure 3.** P4CLS sensitivity to confinement,  $-(\partial \log \tau / \partial (1/h))_T$ , as a function of temperature. The curve is the CFV prediction and the symbols are the experimental results. The inset shows a sketch of how bulk segmental times change with  $V_{\text{free}}$  during pressure ramps in isothermal conditions.

trend has been observed in prior experimental and modeling work,<sup>35–43</sup> however, using the CFV model we are now in a position to provide insight regarding the physical origin of this behavior. There are two contributions: First, this work demonstrates that the CFV model can successfully map the effect of confinement onto the effect of changing free volume, just as it would in bulk  $P$ -dependent dynamics. As sketched in the Figure 3 inset, bulk isothermal relaxation times change less rapidly with, become less sensitive to, changing free volume when at higher temperatures. It follows similarly for films that relaxation times will be less sensitive to isothermal changes in film thickness at high  $T$ , because  $h$  and  $V_{\text{free}}$  are related. (Mechanistically, cooperativity is what causes this  $T$ – $V$  ( $T$ – $h$ ) coupling; see eq 3.) Second, recall that, at constant pressure, as  $T$  increases the (free) volume of a melt will increase. Then, because cooperativity goes as  $n^* \propto 1/V_{\text{free}}$ , its sensitivity to isothermal changes,  $\partial(1/h) \propto \partial V_{\text{free}}$ , will scale as  $(\partial n^* / \partial (1/h))_T \propto -(1/V_{\text{free}})^2$  (see SI). This means the difference in cooperativity,  $\Delta n^*$ , between two films of different thickness,  $\Delta h$ , will be smaller at higher temperature. Therefore, as  $T$  increases the effect of changing film thickness on local

relaxation will become weaker due to decreasing differences in activation energy.

## MATERIALS AND METHODS

Thin films of poly(4-chlorostyrene) ( $M_w = 75,000$  g/mol, PDI = 1.48, powder, Sigma-Aldrich, indicated in the text as P4CLS) were spin cast at 3000 rpm from solutions of the polymer in toluene (99.8% from Sigma) directly onto thermally evaporated aluminum (Aldrich 99.999%, evaporation rate  $\geq 10$  nm s $^{-1}$ , thickness  $\sim 50$ –100 nm) and held for  $>10^4$  times the segmental time,  $\tau$ , at 10 K above bulk  $T_g$ . (The bulk’s dynamic  $T_g$  obtained via the extrapolation of a VFT fit as  $\tau(T_g) = 100$  s is 401 K.) Next, the upper surfaces of the films were metallized (Al, thermal evaporation in the same conditions described for the lower electrode) to permit the application of relatively low voltages to the resulting nanocapacitors. Nanocapacitors fabricated with this model can be treated as a symmetric nanosystem, where polymer slabs are confined within two identical walls. The complex dielectric function was measured in a helium environment using an impedance analyzer (Solatron Analytical) in isothermal conditions. Relaxation processes were analyzed using the empirical Havriliak–Negami (HN) function,<sup>44</sup> which allowed extracting the value of  $\tau$  from the recorded spectra. The results shown in this work correspond to the “0 annealing time” condition described in ref 18, where the degree of irreversible adsorption is lowest and the interfacial free volume content highest; this metastable nonequilibrium state is easily modeled by the value of  $\delta_{\text{free}}$ .

## ASSOCIATED CONTENT

### Supporting Information

The Supporting Information is available free of charge on the ACS Publications website at DOI: [10.1021/acsmacrolett.8b00844](https://doi.org/10.1021/acsmacrolett.8b00844).

Details on model characterization for P4CLS; details on model interpretation of sensitivity to confinement; details on calculations for Figure 3 (PDF).

## AUTHOR INFORMATION

### Corresponding Authors

\*E-mail: [snapolit@ulb.ac.be](mailto:snapolit@ulb.ac.be).  
\*E-mail: [jane.lipson@dartmouth.edu](mailto:jane.lipson@dartmouth.edu).

### ORCID

Jane E. G. Lipson: [0000-0002-0177-9373](https://orcid.org/0000-0002-0177-9373)  
Simone Napolitano: [0000-0001-7662-9858](https://orcid.org/0000-0001-7662-9858)

### Notes

The authors declare no competing financial interest.

## ACKNOWLEDGMENTS

J.E.G.L. and R.P.W. gratefully acknowledge the financial support provided by the National Science Foundation (DMR-1708542). S.N. acknowledges the Fonds de la Recherche Scientifique FNRS under Grant T.0147.16 “TIACIC”.

## REFERENCES

- (1) Napolitano, S.; Glynn, E.; Tito, N. B. Glass transition of polymers in bulk, confined geometries, and near interfaces. *Rep. Prog. Phys.* **2017**, *80*, No. 036602.
- (2) Ediger, M. D.; Forrest, J. A. Dynamics near Free Surfaces and the Glass Transition in Thin Polymer Films: A View to the Future. *Macromolecules* **2014**, *47*, 471–478.
- (3) Richert, R. Dynamics of Nanoconfined Supercooled Liquids. *Annu. Rev. Phys. Chem.* **2011**, *62*, 65–84.

(4) Alcoutabi, M.; McKenna, G. Effects of confinement on material behaviour at the nanometre size scale. *J. Phys.: Condens. Matter* **2005**, *17*, R461–R524.

(5) Simmons, D. S. An Emerging Unified View of Dynamic Interphases in Polymers. *Macromol. Chem. Phys.* **2016**, *217*, 137–148.

(6) Baschnagel, J.; Varnik, F. Computer simulations of supercooled polymer melts in the bulk and in-confined geometry. *J. Phys.: Condens. Matter* **2005**, *17*, R851–R953.

(7) Cangialosi, D.; Alegria, A.; Colmenero, J. Effect of nanostructure on the thermal glass transition and physical aging in polymer materials. *Prog. Polym. Sci.* **2016**, *54–55*, 128–147.

(8) Boucher, V. M.; Cangialosi, D.; Yin, H.; Schoenholz, A.; Alegria, A.; Colmenero, J. T-g depression and invariant segmental dynamics in polystyrene thin films. *Soft Matter* **2012**, *8*, 5119–5122.

(9) Fukao, K.; Miyamoto, Y. Glass transitions and dynamics in thin polymer films: Dielectric relaxation of thin films of polystyrene. *Phys. Rev. E: Stat. Phys., Plasmas, Fluids, Relat. Interdiscip. Top.* **2000**, *61*, 1743–1754.

(10) Kremer, F.; Tress, M.; Mapesa, E. U. Glassy dynamics and glass transition in nanometric layers and films: A silver lining on the horizon. *J. Non-Cryst. Solids* **2015**, *407*, 277–283.

(11) Donth, E. J. *The Glass Transition: Relaxation Dynamics in Liquids and Disordered Materials*; Springer, 2001.

(12) Adam, G.; Gibbs, J. H. On Temperature Dependence of Cooperative Relaxation Properties in Glass-Forming Liquids. *J. Chem. Phys.* **1965**, *43*, 139–146.

(13) Kirkpatrick, T. R.; Thirumalai, D.; Wolynes, P. G. Scaling Concepts for the Dynamics of Viscous-Liquids Near an Ideal Glassy State. *Phys. Rev. A: At., Mol., Opt. Phys.* **1989**, *40*, 1045–1054.

(14) Lubchenko, V.; Wolynes, P. G. Theory of structural glasses and supercooled liquids. *Annu. Rev. Phys. Chem.* **2007**, *58*, 235–266.

(15) Tanaka, H.; Kawasaki, T.; Shintani, H.; Watanabe, K. Critical-like behaviour of glass-forming liquids. *Nat. Mater.* **2010**, *9*, 324–331.

(16) Napolitano, S.; Capponi, S.; Vanroy, B. Glassy dynamics of soft matter under 1D confinement: How irreversible adsorption affects molecular packing, mobility gradients and orientational polarization in thin films. *Eur. Phys. J. E: Soft Matter Biol. Phys.* **2013**, *36*, 61.

(17) Oh, S. H.; Kauffmann, Y.; Scheu, C.; Kaplan, W. D.; Ruhle, M. Ordered liquid aluminum at the interface with sapphire. *Science* **2005**, *310*, 661–663.

(18) Panagopoulou, A.; Napolitano, S. Irreversible Adsorption Governs the Equilibration of Thin Polymer Films. *Phys. Rev. Lett.* **2017**, *119*, No. 097801.

(19) Priestley, R. D.; Cangialosi, D.; Napolitano, S. On the equivalence between the thermodynamic and dynamic measurements of the glass transition in confined polymers. *J. Non-Cryst. Solids* **2015**, *407*, 288–295.

(20) White, R. P.; Lipson, J. E. G. Polymer Free Volume and Its Connection to the Glass Transition. *Macromolecules* **2016**, *49*, 3987–4007.

(21) Napolitano, S.; Rotella, C.; Wubbenhorst, M. Can Thickness and Interfacial Interactions Univocally Determine the Behavior of Polymers Confined at the Nanoscale? *ACS Macro Lett.* **2012**, *1*, 1189–1193.

(22) White, R. P.; Lipson, J. E. G. Connecting Pressure-Dependent Dynamics to Dynamics under Confinement: The Cooperative Free Volume Model Applied to Poly(4-chlorostyrene) Bulk and Thin Films. *Macromolecules* **2018**, *51*, 7924–7941.

(23) White, R. P.; Lipson, J. E. G. Explaining the T,V-dependent dynamics of glass forming liquids: The cooperative free volume model tested against new simulation results. *J. Chem. Phys.* **2017**, *147*, 184503.

(24) White, R. P.; Lipson, J. E. G. How Free Volume Does Influence the Dynamics of Glass Forming Liquids. *ACS Macro Lett.* **2017**, *6*, 529–534.

(25) Roland, C.; Hensel-Bielowka, S.; Paluch, M.; Casalini, R. Supercooled dynamics of glass-forming liquids and polymers under hydrostatic pressure. *Rep. Prog. Phys.* **2005**, *68*, 1405–1478.

(26) Floudas, G.; Paluch, M.; Grzybowski, A.; Ngai, K. *Molecular Dynamics of Glass-Forming Systems - Effects of Pressure*; Springer: Berlin, 2011.

(27) Casalini, R.; Mohanty, U.; Roland, C. M. Thermodynamic interpretation of the scaling of the dynamics of supercooled liquids. *J. Chem. Phys.* **2006**, *125*, No. 014505.

(28) Adrjanowicz, K.; Kaminski, K.; Koperwas, K.; Paluch, M. Negative Pressure Vitrification of the Isochorically Confined Liquid in Nanopores. *Phys. Rev. Lett.* **2015**, *115*, 265702.

(29) Adrjanowicz, K.; Kaminski, K.; Tarnacka, M.; Szklarz, G.; Paluch, M. Predicting Nanoscale Dynamics of a Glass-Forming Liquid from Its Macroscopic Bulk Behavior and Vice Versa. *J. Phys. Chem. Lett.* **2017**, *8*, 696–702.

(30) Tarnacka, M.; Kipnusu, W. K.; Kaminska, E.; Pawlus, S.; Kaminski, K.; Paluch, M. The peculiar behavior of the molecular dynamics of a glass-forming liquid confined in native porous materials - the role of negative pressure. *Phys. Chem. Chem. Phys.* **2016**, *18*, 23709–23714.

(31) Kipnusu, W. K.; Elsayed, M.; Kossack, W.; Pawlus, S.; Adrjanowicz, K.; Tress, M.; Mapesa, E. U.; Krause-Rehberg, R.; Kaminski, K.; Kremer, F. Confinement for More Space: A Larger Free Volume and Enhanced Glassy Dynamics of 2-Ethyl-1-hexanol in Nanopores. *J. Phys. Chem. Lett.* **2015**, *6*, 3708–3712.

(32) Huang, X.; Roth, C. B. Changes in the temperature-dependent specific volume of supported polystyrene films with film thickness. *J. Chem. Phys.* **2016**, *144*, 234903.

(33) Unni, A. B.; Vignaud, G.; Chapel, J. P.; Giermanska, J.; Bal, J. K.; Delorme, N.; Beuvier, T.; Thomas, S.; Grohens, Y.; Gibaud, A. Probing the Density Variation of Confined Polymer Thin Films via Simple Model-Independent Nanoparticle Adsorption. *Macromolecules* **2017**, *50*, 1027–1036.

(34) Zhou, Y.; Milner, S. T. Short-Time Dynamics Reveals T-g Suppression in Simulated Polystyrene Thin Films. *Macromolecules* **2017**, *50*, 5599–5610.

(35) Napolitano, S.; Lupascu, V.; Wubbenhorst, M. Temperature dependence of the deviations from bulk behavior in ultrathin polymer films. *Macromolecules* **2008**, *41*, 1061–1063.

(36) Fakhraai, Z.; Forrest, J. Probing slow dynamics in supported thin polymer films. *Phys. Rev. Lett.* **2005**, *95*, No. 025701.

(37) Peter, S.; Meyer, H.; Baschnagel, J. Thickness-dependent reduction of the glass-transition temperature in thin polymer films with a free surface. *J. Polym. Sci., Part B: Polym. Phys.* **2006**, *44*, 2951–2967.

(38) Shavit, A.; Riggelman, R. A. Influence of Backbone Rigidity on Nanoscale Confinement Effects in Model Glass-Forming Polymers. *Macromolecules* **2013**, *46*, 5044–5052.

(39) Diaz-Vela, D.; Hung, J.; Simmons, D. S. Temperature-Independent Rescaling of the Local Activation Barrier Drives Free Surface Nanoconfinement Effects on Segmental-Scale Translational Dynamics near  $T_g$ . *ACS Macro Lett.* **2018**, *7*, 1295–1301.

(40) Long, D.; Lequeux, F. Heterogeneous dynamics at the glass transition in van der Waals liquids, in the bulk and in thin films. *Eur. Phys. J. E: Soft Matter Biol. Phys.* **2001**, *4*, 371–387.

(41) Merabia, S.; Sotta, P.; Long, D. Heterogeneous nature of the dynamics and glass transition in thin polymer films. *Eur. Phys. J. E: Soft Matter Biol. Phys.* **2004**, *15*, 189–210.

(42) Hanakata, P. Z.; Betancourt, B. A. P.; Douglas, J. F.; Starr, F. W. A unifying framework to quantify the effects of substrate interactions, stiffness, and roughness on the dynamics of thin supported polymer films. *J. Chem. Phys.* **2015**, *142*, 234907.

(43) Phan, A. D.; Schweizer, K. S. Dynamic Gradients, Mobile Layers, T-g Shifts, Role of Vitrification Criterion, and Inhomogeneous Decoupling in Free-Standing Polymer Films. *Macromolecules* **2018**, *51*, 6063–6075.

(44) Havriliak, S.; Negami, S. A Complex Plane Representation of Dielectric and Mechanical Relaxation Processes in Some Polymers. *Polymer* **1967**, *8*, 161–210.